Localization of charge carriers by Pr in the $Tl_2Ba_2Ca_{1-x}Pr_xCu_2O_y$ system

S. N. Bhatia,* P. Chowdhury, S. Gupta, and B. D. Padalia
Department of Physics, Indian Institute of Technology, Bombay 400 076, India
(Received 22 October 2001; revised manuscript received 19 August 2002; published 31 December 2002)

We have measured the resistivity and thermoelectric power of $Tl_2Ba_2Ca_{1-x}Pr_xCu_2O_y$ samples with $x \leqslant 0.6$ in the temperature range 10–300 K. T_c decreases with an increase in the Pr concentration and a crossover from a metallic to insulator state is observed in samples with $x \simeq 0.4$. In the highly resistive samples ($x > 0.4$) conduction is governed by the in-plane variable range hopping of the carriers while in others, localization of bosons appears to be dominating. A ''spin gap'' is observed in the resistivity of these samples. The resistivity and thermoelectric power show the localization of the carriers to increase with an increase in Pr concentration. These data, examined in the light of existing models of conduction by localized carriers, show a preference for the model proposed by Nagaosa and Lee wherein the fermion contribution decreases and that of the bosons increases with the increase in the Pr concentration. The Pr L_3-edge absorption data show Pr to be present in the mixed (3^+ and 4^+) valent state. Correlating the hole density ''p'' determined from T_c and thermoelectric power with the valence of Pr estimated from x-ray-absorption edge measurements, we find hole filling along with hybridization to be the dominant mechanism for destablization and eventual suppression of superconductivity in these materials.

DOI: 10.1103/PhysRevB.66.214523 PACS number(s): 74.72.Fq, 74.25.Fy, 74.62.Dh

I. INTRODUCTION

In recent years, rare-earth substitutions in high-temperature superconductors (HTS) have attracted considerable attention. Pr substitution at the Ca site in $Bi_2Sr_2CaCu_2O_8$ (BSCCO) (Refs. 1 and 2) were found to localize the carriers, with increasing Pr concentration, and lead to the suppression of superconductivity for Pr concentration exceeding a certain critical value x_c. At higher concentrations of Pr, conduction was observed to take place by the variable range hopping (VRH) of the carriers which changed character from being two dimensional near the superconductor - insulator boundary ($x \sim x_c$) to three dimensional far above it. Of all the rare-earth metals, Awana *et al.*[1] found both Pr and Ce to be most effective in suppressing the superconductivity due to the hole-filling mechanism, since both these ions were found to exist in the tetravalent state. Further substituting Y for Ca in $Tl_2Ba_2CaCu_2O_8$ (TBCCO), Poddar *et al.*[3] found Y to behave identically to Pr in BSCCO in suppressing superconductivity and localizing the carriers. However, the localization for Y substitution must be fundamentally different since Y does not have any $4f$ electrons.

In $YBa_2Cu_3O_7$ (YBCO), where Pr substitution also suppresses superconductivity, three mechanisms have been proposed.[4,5] The first involves the breaking of the superconducting pairs by the magnetic moment carried by Pr which causes the scattering of the holes within the CuO_2 planes to be spin dependent. According to the second mechanism, Pr exists in a higher valence state than those of the ions it displaces and acts as a donor of electrons, thereby filling the holes available for conduction in the *ab* planes. The third mechanism involves the hybridization of the Pr (4+) orbital with the O-$2p$ state which leads to the localization of the holes without a significant change in the total hole concentration. Neumeier *et al.*[4] and Norton *et al.*[5] studied these mechanisms in YBCO by substituting both Pr and Ca at the Y site. They found all three mechanisms to be operative. The former ion acts as a donor, and the latter acts as the acceptor of electrons because of its valence is lower than that of Y. The magnetic moment of Pr was also found to facilitate pair breaking. Using the resistivity and thermopower data on $Pr_xY_{1-x}Ba_2Cu_3O_{7-\delta}$, Goncalves *et al.*[6] concluded the band filling to be responsible for suppression of superconductivity in YBCO. From NMR measurements on $PrBa_2Cu_3O_7$, Reyes *et al.*[7] found hole filling as well as pair breaking to be operative while in (R-Pr)$Ba_2Cu_3O_7$ (R=Sm, Gd, Tm), Malik *et al.*[8] and Xu and Guan[9] found hybridization to dominate. It is therefore of interest to see which of these mechanisms are operative in TBCCO.

Further, since its identification by Anderson, much work has been reported on the resonating-valence-bond model. Nagaosa and Lee[10] have shown that below their condensation temperature, a ''gap'' appears in the spectrum of bosons which manifests itself in the electric and thermal conduction. The dependence of resistivity on temperature becomes significantly different from that proposed by Anderson.

In order to examine the proposed mechanisms, we have substituted Pr at the Ca site in TBCCO. We find this substitution to increase the localization, leading to a metal-to-insulator transition for sheet resistance exceeding the critical value proposed by Fisher *et al.*[11] We also find conduction by VRH to be prevalent in insulating samples, but in superconducting samples ($x \leqslant x_c$), we observe a ''spin gap'' in their normal-state resistivity and conduction to take place by charged bosons following the model proposed by Nagaosa and Lee.[10] Correlating the hole density ''p'' determined from T_c and thermoelectric power (TEP) with the valence of Pr estimated from x-ray-absorption edge measurements, we find hole filling along with hybridization to be the dominant mechanism operating in these samples. The results of such investigations are discussed here.

II. EXPERIMENTAL DETAILS

The conventional powder-metallurgy approach, that of mixing and heating the constituent oxides and carbonates,

TABLE I. T_c, p, the oxygen content of the molecules, and residual sheet resistance $\rho_\square$ for different concentrations of Pr and x. $y(Pr^{3+})$ and $y(Pr^{4+})$ were calculated for Pr in 3+ and 4+ valent states, respectively.

x	T_c (K)	p	y_T	$y(Pr^{3+})$	$y(Pr^{4+})$	$\rho_\square$ (kΩ)
0.0	97.5	0.20	8.13±0.01	8.16	8.16	
0.05	95.0					
0.1	85.7	0.12	8.18	8.17	8.22	3.87
0.2	52.0	0.08	8.19	8.18	8.28	6.61
0.4	15.2	0.06	8.34	8.26	8.46	11.7
0.6	⩽10	0.05	8.34	8.35	8.65	

Tl_2O_3, $BaCO_3$, $CaCO_3$, and CuO, does not succeed in the synthesis of $Tl_2Ba_2CaCu_2O_{8+\delta}$ superconductors due to the high volatility of Tl_2O_3 at the reaction temperature. Tl_2O_3 decomposes above 850 °C to Tl_2O, which melts at 300 °C. The problem of Tl loss can be significantly curbed by using the precursor matrix reaction method.[12] A precursor with the composition $Ba_2Ca_{1-x}Pr_xCu_2O_{5+\delta}$ was prepared by calcining stoichiometric mixtures of $BaCO_3$, $CaCO_3$, Pr_6O_{11}, and CuO at 850 °C for 24 h in air. The product was then ground and fired at 930 °C for 24 h in order to facilitate the completion of the reaction. $Ba_2Ca_{1-x}Pr_xCu_2O_{5+\delta}$ was mixed with Tl_2O_3 in the molar ratio 1:1, ground, and pressed into pellets. The pellets were kept inside a vertical furnace, preheated to 810 °C, for 10 min under oxygen flow and then furnace cooled to room temperature. After grinding and repelletizing, the pellets were heated again at the same temperature for an increased duration (~1 hr) under oxygen flow. The samples were characterized by the powder x-ray diffractometry using Cu $K\alpha$ radiation. The oxygen content, ''y,'' of these samples was measured by the standard iodometric titration method and is listed as Y_T in Table I. ac susceptibility was measured to check the stratification of oxygen in the samples. A single peak with a width of ~5 K was observed in χ'' which indicates the oxygen to be distributed reasonably uniformly within the sample.[13] The temperature dependence of dc resistivity of rectangular-shaped samples was measured by a standard four-probe technique in the temperature range 10–300 K. A closed-cycle refrigerator was used for cooling the samples while their temperatures were monitored with a silicon-diode sensor. TEP was measured by a dc differential method in the same temperature range. Care was taken to use the same pellet for both measurements. The temperature gradient across the sample was measured using two pairs of copper-constantan thermocouples. The sample was mounted with low-temperature epoxy on top of two well-separated copper blocks. Strain gauges were attached to these blocks and were used as heaters to create the desired temperature gradient. By reversing the gradient, the thermally generated spurious voltages could be compensated. The temperature gradient between the two blocks was kept at 0.5 K. To eliminate the effect of the reference leads, the absolute thermoelectric power of Cu was subtracted from the measured thermoelectric voltage. The entire measurement system, comprised of two 181 Keithley nanovoltmeters, a 224 Keithley current source, and a Lakeshore temperature controller,

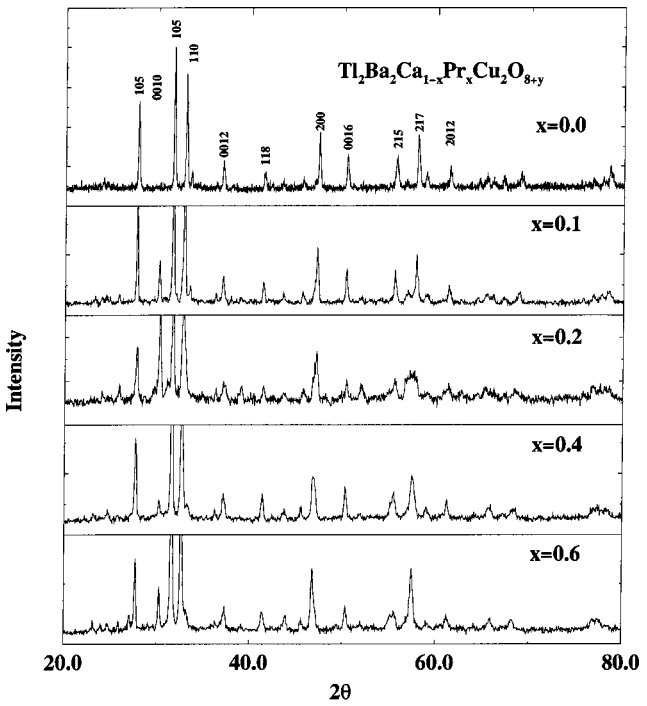

FIG. 1. Powder x-ray-diffraction patterns for $x=0$, 0.1, 0.2, 0.4, and 0.6 in the $Tl_2Ba_2Ca_{1-x}Pr_xCu_2O_y$ samples.

was interfaced with a personal computer for automatic data acquisition.[14] X-ray-absorption measurements on the Pr L_3 and Cu K absorption edges were made with a focusing spectrograph using a laboratory source of x rays. Spectra were collected at room temperature on finely powdered samples mounted on adhesive tape. The spectra were background subtracted and normalized. The details of the spectrograph and the normalizing procedure are discussed elsewhere.[15]

III. RESULTS AND ANALYSIS

The x-ray-diffraction (XRD) patterns of $Tl_2Ba_2Ca_{1-x}Pr_xCu_2O_y$ [TBC(Pr)CO], are shown in Fig. 1 for all the dopant concentrations studied. All samples are single phase. The XRD patterns were indexed with a tetragonal unit cell and space group $I4/mmm$. The variation of the lattice parameters ''a'' and ''c'' with the dopant concentration is shown in Fig. 2. The a-axis parameter increases, while the c-axis length decreases after an initial increase with x. The decrease in c can arise due to (i) an increase in the oxygen content, (ii) substitution of a higher valence cation, or (iii) substitution of a cation with an ionic radius smaller than that of Ca^{2+} with eightfold coordination. The eightfold coordinated ionic radius of Ca^{2+} is 1.12 Å, while for Pr^{3+} and Pr^{4+} it is 1.126 and 0.96 Å, respectively. The oxygen content of these samples increases with x up to $x \leqslant 0.4$ beyond which it saturates (Table I). Apparently all these effects contribute to the observed reduction in c.

The Pr L_3 absorption edge spectra for the $x=0.4$ and $x=0.6$ samples are shown in Fig. 3. The spectrum of the reference compound Pr_6O_{11} is also included for comparison. Our spectrum of Pr_6O_{11} is similar to that reported by Gas-

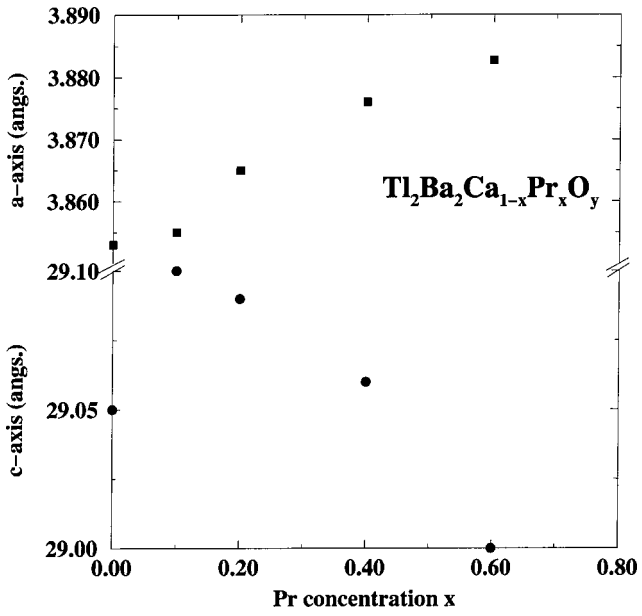

FIG. 2. The variation of the lattice parameters "*a*" and "*c*" with x in $Tl_2Ba_2Ca_{1-x}Pr_xCu_2O_y$ samples.

gnier *et al.*[16] The spectral features of the $x=0.4$ and $x=0.6$ samples given in Fig. 3 resemble with those of Pr_6O_{11}. This suggests that Pr in $x=0.4$ and 0.6 samples is present in 3^+ as well as 4^+ valence states. Further, through the Cu *K*-edge measurements, Cu was found predominantly in the divalent state in these samples.

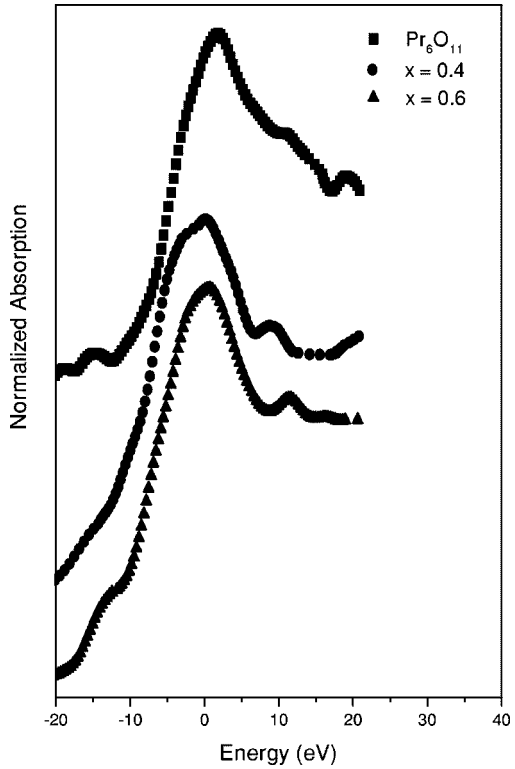

FIG. 3. Pr L_3 absorption spectra for (a) Pr_6O_{11} and $Tl_2Ba_2Ca_{1-x}Pr_xCu_2O_y$ samples with $x=0.4$ and $x=0.6$. The origin of energy is set at the main peak of Pr_6O_{11}. The curves have been shifted vertically for clarity.

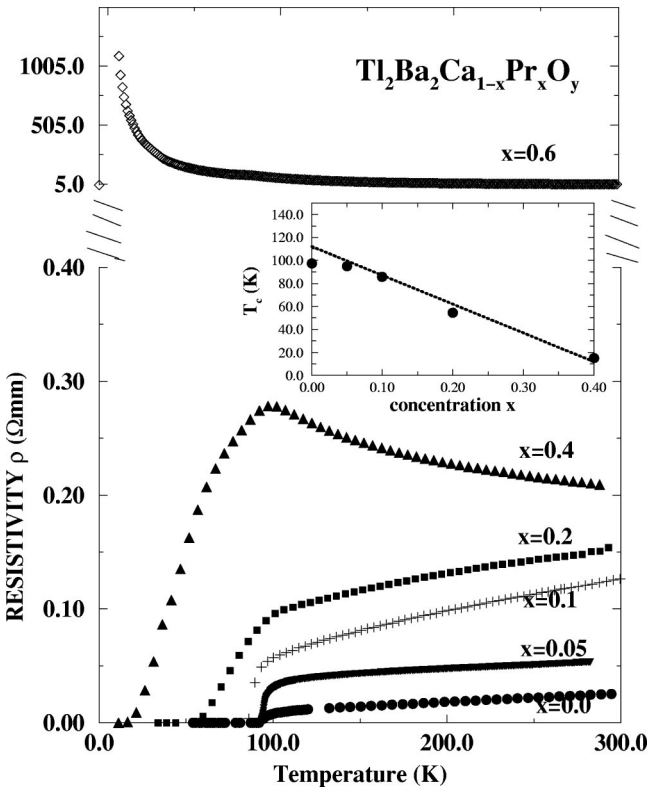

FIG. 4. The temperature dependence of resistivity for $Tl_2Ba_2Ca_{1-x}Pr_xCu_2O_y$ samples with $0 \leqslant x \leqslant 0.6$. The figure in the inset shows the variation of T_c with x. The (dashed) line is a guide to the eye to indicate the linear variation of T_c at large x.

A. Analysis of resistivity and TEP data of superconducting TBC(Pr)CO samples, $x \leqslant 0.2$

Figure 4 shows the temperature dependence of resistivity for TBC(Pr)CO with $x \leqslant 0.6$. With an increase of Pr concentration, the absolute value of the resistivity in the normal state (ρ_n) increases and the transition temperature $T_c(\rho=0)$ gradually decreases. For $x \leqslant 0.2$, the temperature coefficient of resistivity, $d\rho/dT$, is always positive, indicating a metallic conduction. For samples $x=0.4$ and 0.6, resistivity at high temperatures is semiconductorlike with $d\rho/dT$ being negative up to ~ 100 K. For $x=0.4$ a superconducting state with an onset at ~ 100 K sets in, but for $x=0.6$ the semiconducting behavior continues up to the lowest temperature measured (~ 10 K). The variation of $T_c(\rho=0)$ with x is shown in the inset of Fig. 4. T_c decreases with the incorporation of Pr in the lattice. The critical concentration at which superconductivity disappears is ~ 0.45. The behavior observed here is similar to that observed in BSCCO by Awana *et al.*[1] where superconductivity was seen to be completely suppressed for Pr concentrations of ~ 0.4 and the material became semiconducting for $x \geqslant 0.5$. However, it is noted that the resistivity of the present samples is much lower than those of the corresponding BSCCO samples for the same level of Pr substitutions. Further it can be seen from the figure that T_c varies nonlinearly with x at small x and linearly at large x. The linear part, when extrapolated to $x \to 0$, gives an intercept of 112 ± 2 K which is also the maximum T_c observed for this series.[17]

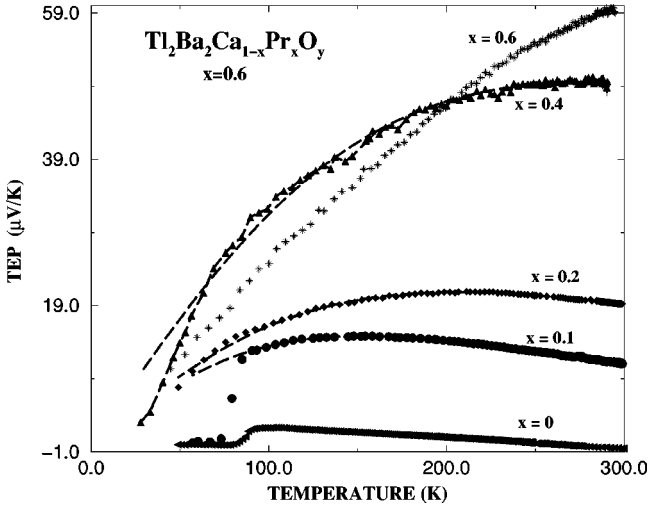

FIG. 5. Temperature dependence of the thermopower (S) for $Tl_2Ba_2Ca_{1-x}Pr_xCu_2O_y$ samples with $0 \leqslant x \leqslant 0.6$. The dashed curves are the predictions of the Nagaosa and Lee model, Eq. (5).

The thermoelectric power (S) for all the samples is plotted in Fig. 5. For the undoped sample ($x=0.0$), S is small in magnitude and shows an almost linear variation with temperature with a negative slope (dS/dT) up to ~100 K below which it passes through a maximum and then falls rapidly to zero at the transition temperature. It shows a positive thermopower in the temperature range 100–200 K and is negative above this temperature. With the incorporation of Pr, the variation of TEP with T becomes nonlinear. The S vs T curves become convex and their convexity increases with the increase in Pr concentration. The temperature at which S attains its maximum value also shifts to higher values. The behavior of S observed here is qualitatively similar to that observed by Goncalves *et al.*[6] in $Pr_xY_{1-x}Ba_2Cu_3O_{7-\delta}$.

Obertelli *et al.*[18] observed that the room-temperature value of TEP (S_{RT}) of various high-T_c cuprates follows a universal dependence on the density of holes in the Cu-O planes, p, and T_c/T_c^{max} in both the underdoped as well as the overdoped regions. T_c^{max} here is the maximum T_c observed for the particular series. According to this behavior, S_{RT} is negative for the overdoped samples only. It is positive and increases with decreasing p for the underdoped samples. Interestingly the present samples appear to follow this universal behavior since S_{RT} of all the samples falls on these curves for the value of T_c^{max} determined above. Since the TEP of the undoped sample ($x=0$) is negative in the neighborhood of room temperature, it is overdoped while all the Pr-doped samples are underdoped because their S_{RT}'s are positive. Underdoped samples have characteristically large and positive values of TEP with a dependence on T of the type observed here for Pr-doped samples. We have determined p from these universal curves for all Pr concentrations and have listed the same in Table I. p is observed to decrease with increasing x. This suggests that holes are being removed by Pr. With these values of T_c^{max} and p, T_c follows the universal relation proposed by Presland *et al.*[19] for the cuprates:

$$T_c = T_c^{max}[1-82.6(p-0.16)^2]. \quad (1)$$

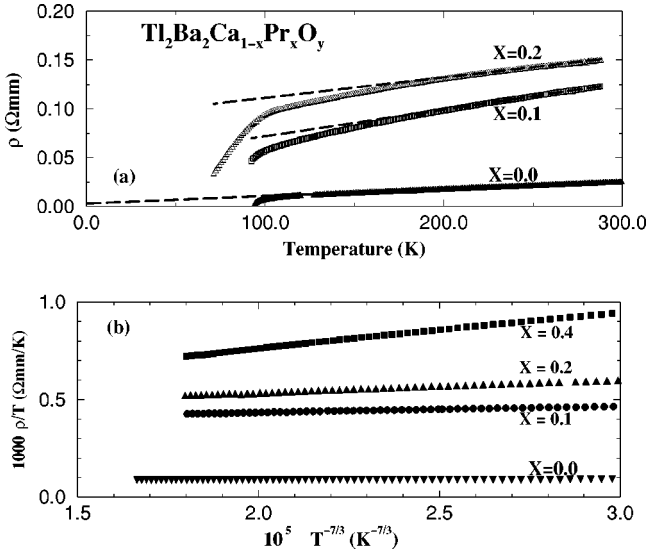

FIG. 6. (a) The presence of a pseudogap in these samples and (b) agreement of the resistivity data with the Nagaosa and Lee model, Eq. (2).

This is a parabolic relation, showing a gradual decrease of T_c at small p and essentially a linear decrease at large p. Poddar *et al.*[3] studied the effect of Y doping in TBCCO. They have also measured the Hall coefficient in TBC(Y)CO and found the concentration of mobile holes to decrease as x increases. They also found p to increase at first nonlinearly with x and then linearly at large x. A similar quadratic relation between T_c and x was also found in $Y_{1-x-y}Ca_yPr_xCu_3O_{7+\delta}$ by Neumeier *et al.*[4] The observation of an initial nonlinear variation of T_c with x in the present samples is an important result, since it suggests that the magnetic moment of Pr ions may not be responsible for the suppression of superconductivity. According to the pair-breaking theory of Abrikosov and Gorkov,[20] T_c is expected to decrease linearly with x for low concentrations of the magnetic impurities.

It is to be noted that even though the $x \leqslant 0.2$ samples show a positive $d\rho/dT$, their resistivities do not follow a linear relation ($\rho = A + BT$) over the entire range of temperatures (100–300 K). They are linear above ~200 K only and deviate rather sharply from this behavior below 200 K, as shown in Fig. 6(a). A linearly decreasing ρ in the room-temperature region is a common feature observed in the cuprates and has been ascribed to the HTS being ''good metals.'' However this behavior contrasts sharply with that observed from TEP. For good metals, Mott's formula predicts TEP to decrease essentially linearly with temperature whereas it is observed to increase with T in the present samples. Such an increase is predicted for the semiconducting samples or for materials having localized states near the Fermi level.[21] A few phenomenological models have also been proposed by, e.g., Gottwick *et al.*[22] and Gasumyants *et al.*,[23] which take this localization into account by superimposing a narrow band of localized states on a fairly wide conduction band. As shown in Fig. 7, the TEP for the present samples follows these models adequately and the localized band gets progressively filled[14] suggesting thereby the localization to increase with

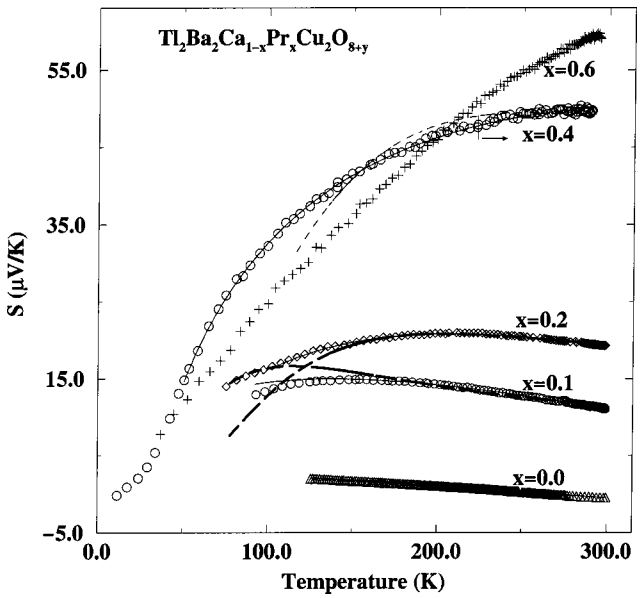

FIG. 7. Best-fit curves for $Tl_2Ba_2Ca_{1-x}Pr_xCu_2O_y$ ($0 \leqslant x \leqslant 0.6$) samples. The dashed lines depict the predictions of the Gottwick *et al.* model (Ref. 22) and the solid lines of the Gasumyants *et al.* model (Ref. 23).

the Pr concentration. Deviations from linearity in the resistivity data similarly point towards the presence of localized states. In our opinion this data should not be bifurcated into ''metallic'' and ''nonmetallic'' ranges. Instead it should be analyzed in one range starting from room temperature and extending up to the onset temperature of superconductivity. A similar sharp departure from linearity was also seen in the resistivity data of $Y_{1-x}Pr_xBa_2Cu_3O_7$ (Y(Pr)BCO) by Liu and Guan[24] and attributed to the opening of a ''spin gap.'' The gap width was seen to increase with Pr concentration. The onset temperature T_s and the width of the gap Δ are both related to the hole/carrier density. The values of Δ in the present samples are about the same as observed in Y(Pr)BCO ($\sim$200 K), but they do not vary as rapidly with x as they do in Y(Pr)BCO. In the Pr-free samples, the resistivity remains linear right down to $\sim$120 K. The onset of the gap (if any) there appears to be masked by the thermal fluctuations which appear at around the same temperature.[25] It may be pointed out that a linearly varying $\rho(T)$ at high temperatures can also result from the scattering of electrons by phonons, but such a process gives a concave $\rho(T)$ vs T curve (Bloch-Gruniesen relation) whereas the shapes of the curves in the present case are distinctly convex.[14]

Nagaosa and Lee[10] have suggested that the anomalous normal-state properties of high-T_c cuprates can be explained by using a variation in the uniform resonating-valence-bond (RVB) model in which fermions and spinless bosons are coupled by a gauge field. A spin gap opens due to the pairing of the fermions at temperatures above the condensation temperature, T_D^0, of the holons. The system behaves like a nondegenerate semiconductor instead of a metal. The resistivity equals the sum of the boson (ρ_B) and fermion (ρ_F) resistivities. Since at high temperatures, ρ_B varies as T and ρ_F as $T^{-4/3}$ the net resistivity $\rho(T)$ is expected to vary as

TABLE II. Parameters obtained by fitting resistivity data to the Nagaosa and Lee model, Eq. (2).

x	A ($\mu\Omega$ cm K^{-1})	B ($\mu\Omega$ cm K$^{4/3}$)	T_L (K)
0 (as prepared)	31	0.28	260
0.1	8	1.3	240
0.2	4	1.8	220

$$\rho(T) = (AT + BT^{-4/3}). \tag{2}$$

Further since $\rho_B \gg \rho_F$, $\rho(T)$ will generally vary linearly with T. The convexity in ρ then arises due to the opening of the spin gap. Its onset temperature T_s will increase as T_D^0 increases with decreasing hole concentration. The data of the superconducting samples follows this equation at temperatures $T > 2T_c$ only. The plots of $\rho(T)/T$ vs $T^{-7/3}$ are shown in Fig. 6(b). As seen here these plots become linear above 200 K for all samples with $x \leqslant 0.2$. The values of the coefficients A and B and the temperature T_L above which the linearity begins are given in Table II. T_L is observed to decrease with increasing x. This suggests that the undoped sample may follow Eq. (2) above $\sim$300 K. Nagaosa and Lee have further found that in TEP also, the contributions of bosons and holons are additive, $S = S_B + S_F$, with

$$S_B = \frac{k_B}{e}\left[1 - \ln\left(\frac{2\pi p}{m^* k_B T}\right)\right] \tag{3}$$

and

$$S_F = -\left(\frac{k_B}{e}\right)\frac{k_B T}{E_F}, \tag{4}$$

where m^* is the mass of the boson. With these values, S can be rewritten as

$$S = \frac{k_B}{e}\left[1 - F \ln\frac{2\pi p G}{T} - \frac{T}{H}\right], \tag{5}$$

where $G = 1/m^* k_B$, $H = E_F/k_B$, and $F = 1$. As shown in Fig. 5, this model agrees well with the data over an extended range of temperatures for all concentrations of Pr ($x < 0.2$) with the values of the parameters given in Table III. Chen *et al.*[26] and Keshri *et al.*[27] have also found similar agreement of their TEP data on Pr-doped BSCCO and Y-doped TBCCO

TABLE III. Parameters F, H, and G obtained by fitting TEP data to the Nagaosa and Lee model, Eq. (5).

x	F	H (K)	G (K)
0 (as prepared)	0.0131 ± 0.002	4148 ± 110	$(7.2 \pm 1.0) \times 10^{24}$
0.1	0.112 ± 0.006	1229 ± 40	$(8.4 \pm 0.2) \times 10^4$
0.2	0.242 ± 0.01	851 ± 20	1760 ± 100
0.4	0.393 ± 0.03	880 ± 5	362 ± 4
0.6	0.420 ± 0.01	1256 ± 25	407 ± 10

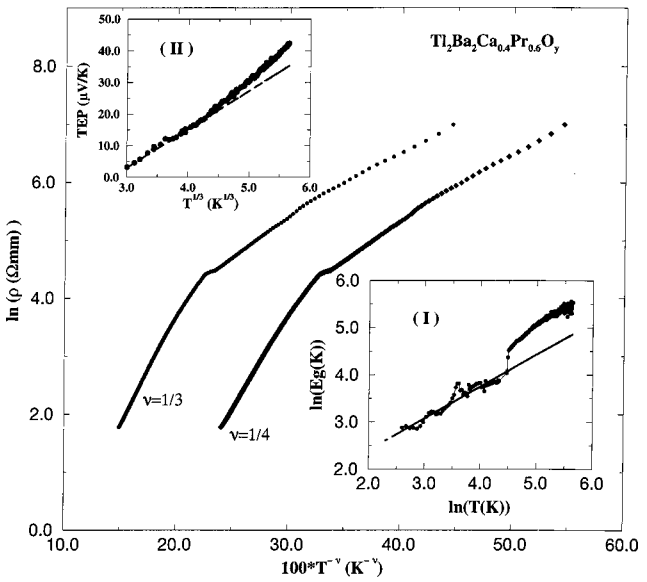

FIG. 8. A plot of $\ln(\rho)$ vs $T^{-\nu}$ for the $Tl_2Ba_2Ca_{1-x}Pr_xCu_2O_y$ sample with $x=0.6$. Inset I shows the variation of the ''activation energy'' E_g with temperature. The (dashed) line drawn through the data at low temperatures corresponds to $\nu \sim 1/3$. Inset II shows that the TEP follows the 2D variable-range-hopping model at low temperatures in the $x=0.6$ sample. The (dashed) line is a guide to the eye.

samples, respectively, and the same has occurred for Ikegawa *et al.*[28] in Eu- and Y-doped electron superconductor $(NdCe)_4(BaSr)_4Cu_6O_y$. In the present samples both resistivity and TEP data are consistent in showing that the fermion contribution decreases and that of the bosons increases as the concentration of Pr increases in these samples.

B. Analysis of resistivity and TEP data of nonsuperconducting TBC(Pr)CO samples, $x \geq 0.4$

The sample with Pr concentration $x=0.6$ shows a resistivity varying as $\exp(T_0/T)^{\nu}$ at low temperatures. A temperature-dependent resistivity of the form

$$\rho(T)=\rho_0 \exp\left(\frac{T_0}{T}\right)^{\nu} \tag{6}$$

generally indicates a conduction by variable range hopping by polarons.[21] The exponent ''ν'' in this equation depends crucially on the behavior of the density of states (DOS) with energy near the Fermi level and the dimensionality ''d'' of the system. For an $(E\text{-}E_F)^m$ dependence of the DOS on energy, $\nu=(m+1)/(m+d+1)$.[29] Thus ν equals 1/3 or 1/4 for hopping in two or three dimensions, respectively, when the DOS remains finite $(m=0)$ at the Fermi level. In Fig. 8, we have plotted $\ln\rho$ vs $T^{-\nu}$ in the temperature range 10–300 K for both $\nu=1/3$ and $\nu=1/4$ for this sample. As is clear from the figure, below ~ 60 K, both values of ν appear to be equally acceptable to the data since both plots appear to be approximately linear but deviate at higher temperatures. In this model, the ''activation energy,'' E_g, defined as $d\ln\rho/d(1/T)$, is expected to vary as $T^{1-\nu}$ and provides another method from which to choose between the two values of ν. We have obtained E_g by numerically differentiating the resistivity data and have shown it as inset I in Fig. 8, by plotting it on a log-log graph. Below ~ 60 K, though the scatter in the data is large, still a straight line with a slope 0.65 corresponding to $\nu \sim 0.35 \simeq 1/3$ can be passed through it. Above this temperature the plot shifts upwards, its slope increases, and a single value of ν cannot be obtained. The measured resistivity when divided by $\exp(1/T)^{1/3}$, which corresponds to the value $\rho_0\exp(T_0)^{1/3}$, is not constant indicating that the characteristic temperature, T_0, is not temperature independent above ~ 60 K. This is also supported by the TEP data. Within the VRH model, TEP is expected to vary as[29]

$$S \propto T^{(d-m-1)/(d+m+1)}, \tag{7}$$

which shows that for $d=2$ and 3, S should vary as $T^{1/3}$ and $T^{1/2}$, respectively, for an energy-independent DOS. The S vs $T^{1/3}$ plot for this sample is also shown in Fig. 8 as inset II. The data appears to follow this behavior below ~ 80 K. Above this temperature though the plot still appears to be linear but the agreement is not as good as it is for the data below 80 K. Also the slope of this straight line changes at this temperature. Because the slope in Eq. (7) is proportional to $T_0^{2/3}$, this change in the slope therefore reflects the value of T_0 to increase at 80 K. The value of E_g determined here, though appropriate for hopping at low temperatures, is small $(\sim 20$ K). It compares favorably with its value determined in single crystals of BSCCO.[30] The localization length estimated from this value, using the DOS determined from the specific heat measured by Junod *et al.*[31] for undoped TBCCO, works out to be ~ 22 Å.

It appears that only those samples which do not attain superconductivity upon cooling conduct by variable range hopping. For the sample with $x=0.4$, though the resistivity appears to follow the VRH process equally well for both values of ν [at temperatures above the onset temperature of superconductivity $(\sim 120$ K)], E_g obtained from it does not support it as it gives a fairly large value for $\nu \sim 0.8$. TEP also does not decrease either as $T^{1/3}$ or as $T^{1/2}$, as is expected for the two-dimensional (2D) and three-dimensional (3D) systems. Conduction here obeys the Nagaosa and Lee model. The resistivity shows linear plots for $\rho(T)/T$ vs $T^{-7/3}$ above 220 K as shown in Fig. 6(b), while TEP fits Eq. (5) down to ~ 120 K, Fig. 5. The $x=0.6$ sample on the other hand does not follow this model since the $\rho(T)/T$ vs $T^{-7/3}$ plots are not linear over any significant interval of temperature.

It may be pointed out that generally resistivity and TEP data in polycrystalline samples do not agree in the same model,[6] since the heat current is expected to be much less sensitive to the porosity and other weak links present in these samples than the charge current.[18] From this point of view the present samples appear to be less porous and also have grains large in size. Underdoping results in creation of oxygen vacancies in the samples. As is argued below, oxygen deficiency in the present samples increases with the incorporation of Pr in the lattice. Localization of the carriers observed here may result from the disorder created by these

vacancies within the conduction layer. It was realized early in the studies of localization[32] in 2D systems that at $T=0$, all single electron states at Fermi levels of these systems were localized irrespective of the strength of disorder present in them. However a metallic conductivity can still be seen if the ''sheet resistance'' of the samples is less than $h/4e^2 = 6.5\ \mathrm{k}\Omega$.[11] This quantity is a universal number and does not depend on the nature of disorder that drives the localization. The more recent scaling theories of localization further predict[33] an insulator-to-superconductor transition for $0.06 \leqslant p \leqslant 0.2$ and a normal-metal-to-superconductor transition for $p \geqslant 0.2$. These predictions can be verified from the in-plane resistivity, ρ_{ab}, of the samples. We have attempted to estimate this resistivity for the doped samples from that measured on the polycrystalline samples using a model of conduction through grains developed by Veira and Vidal[34] and used by the authors[35] to analyze the fluctuation conductivity of polycrystalline BSCCO. This model takes into account the orientational randomness of the *ab* planes of the grains present in the polycrystalline samples through a geometric factor ''*g*'' and the intergrain conduction by including the grain-boundary resistivity ρ_{gb},

$$\rho(T) = \left[\frac{\rho_{ab}(T)}{g} + \rho_{gb} \right]. \tag{8}$$

In the room-temperature region, since $\rho(T)$ decreases linearly with *T*, it implies that ρ_{gb} will also decrease linearly with *T*. By taking $\rho_{gb} = \rho_{0g} T$ and using the $\rho_{ab}(T)$ measured on single crystals[14] we have determined *g* for the undoped TBCCO. Since the doped samples have also been prepared under conditions identical to those of the undoped samples, their microstructures are expected to be identical to those of the undoped samples. *g* is therefore expected to remain unchanged with doping. However, ρ_{0g} will increase with *x* as $\rho(T)$ increases with it. Assuming ρ_{0g} increases at the same rate as that of $\rho(T)$, ρ_{ab} of these samples can be calculated by using the value of *g* determined above. By extrapolating this resistivity to $T \to 0$, the residual resistivity can be obtained from which the sheet resistance $\rho_{\square}$ of the double layer can be calculated by dividing it by the distance between the layers (~ 15 Å).

We have listed these values in Table I. For $x = 0.4$ and 0.6, room-temperature values of $\rho_{\square}$ are given since the extrapolation of $\rho(T)$ to $T \to 0$ is not possible. For the single crystal, $\rho_{\square}$ is $\sim 20\ \Omega$ and is much less than its corresponding value for BSCCO.[30]

From Table I it is seen that $\rho_{\square}$ increases with *x* but remains less than the critical value 6.5 kΩ for $x \leqslant 0.2$. These samples exhibit metallic conductivity (at high temperatures). For $x = 0.4$, $\rho_{\square}$ is greater than the critical value, and this sample exhibits a nonmetallic conductivity.

A decrease in *p* with incorporation of Pr needs some discussion. The decrease of *p* with *x* suggests that Pr ions are effectively filling the holes. As is expected, due to their higher valence [in comparison to the valence of the ions (Ca^{2+}) that they are replacing], Pr ions will release more electrons into the lattice. Since the oxygen content *y* of the molecules is also increasing, some of these electrons are likely to be ''taken up'' by the oxygen ions. For a fixed valence of Pr, 3^+ or 4^+, a simple calculation of the oxygen content that a molecule requires to have the observed value of *p* (Table I), assuming Tl, Ba, and Ca to be present in their nominal valence states, shows that the *y* required for the valence 3^+ [i.e., $y(Pr^{3+})$] is much closer to the experimentally determined values of *y*, thus suggesting Pr to be present in the mixed, 3^+ and 4^+ valent states. This inference agrees with the result obtained from the x-ray-absorption data which also show Pr to be present in the mixed-valent state. In the 3^+ state, Pr has a large ionic radius and can provide a large overlap between the wave functions of its $4f$ electrons with the wave functions of the neighboring copper and oxygen ions. At the same time, being in the higher valence state (4+), Pr will release more electrons. This indicates that the electrons attached to the Pr^{3+} state may be hybridizing with the surrounding ligands and losing their mobility while those originating from Pr^{4+} may be filling the holes. This suggestion is in line with a recent calculation of electronic structure of $PrBa_2Cu_3O_7$ by Fehrenbacher and Rice,[36] wherein they have shown that the suppression of superconductivity results due to the existence of a local $4f - \mathrm{Pr} - 2p_\pi - \mathrm{O} - \mathrm{Pr}^{(IV)}$ hybridized state.

IV. CONCLUSION

The analysis of the data on $Tl_2Ba_2Ca_{1-x}Pr_xCu_2O_y$ shows that the carriers are localized and their numbers are reduced as the concentration of Pr in the samples is increased. This implies that the hole which was originally in the Cu-O plane and was mobile is now transferred to Pr and has become immobile because of a lack of any conducting path within the plane containing Pr. This contention is in line with an earlier suggestion that the hybridization of the Pr-$4f$ state with the O-$2p$ state results in the localization and reduction in the density of mobile holes. The mixed- (3^+ and 4^+) valent nature of Pr suggests that the electrons of the Pr^{3+} state hybridized with surrounding ligands lose their mobility while those of Pr^{4+} are filling the holes, supporting the recent work of Fehrenbacher and Rice.[36] The transport data appears to prefer the model proposed by Nagaosa and Lee,[10] since it predicts correctly the temperature dependence of resistivity and thermoelectric power as well as the ''spin gap'' that is observed by us in the resistivity data. It is seen that the fermion contribution decreases and that of the bosons increases with Pr concentration. Further, it is found when the residual sheet resistance exceeds the critical value proposed by Fisher *et al.*,[11] this model breaks down and conduction takes place by the conventional Mott's variable range hopping process.

ACKNOWLEDGMENTS

The authors would like to thank Professor P.P. Singh for a critical review of the manuscript and gratefully acknowledge the help given by Niharika Mohapatra in computing.

*Corresponding author. FAX: 91-22-5723480. Email address: snbhatia@phy.iitb.ac.in

[1] V.P.S. Awana, S.K. Agarwal, A.V. Narlikar, and M.P. Das, Phys. Rev. B **48**, 1993 (1211).

[2] H.C. Ku, Y.M. Wan, Y.Y. Hsu, S.R. Lin, and D.Y. Hsu, in *Proceedings of the 21st International Conference on Low Temperature Physics, Prague, 1996*, edited by W. Trzeciakowski (World Scientific, Singapore, 1996).

[3] A. Poddar, P. Mandal, A.N. Das, and B. Ghosh, Phys. Rev. B **44**, 2757 (1991).

[4] J.J. Neumeier, T. Bjrnholm, M.B. Maple, and I.K. Schuller, Phys. Rev. Lett. **63**, 2516 (1989).

[5] D.P. Norton, D.H. Lowndes, B.C. Sales, J.D. Budai, E.C. Jones, and B.C. Chakoumakos, Phys. Rev. B **49**, 4182 (1994).

[6] A.P. Goncalves, I.C. Santos, E.B. Lopes, R.T. Henriques, M. Almeida, and M.O. Figueiredo, Phys. Rev. B **37**, 7476 (1988).

[7] A.P. Reyes, D.E. MacLaughin, M. Takigawa, P.C. Hammel, R.H. Heffner, J.D. Thompson, J.E. Crow, A. Kebede, T. Minalisin, and J. Schwegler, Phys. Rev. B **42**, 2688 (1990).

[8] S.K. Malik, C.V. Tomy, and Parag Bhagava, Phys. Rev. B **44**, 7042 (1991).

[9] Yunhui Xu and Weiyan Guan, Phys. Rev. B **45**, 3176 (1992).

[10] N. Nagaosa and P.A. Lee, Phys. Rev. Lett. **64**, 2450 (1990); Phys. Rev. B **45**, 966 (1992).

[11] M.P.A. Fisher, G. Gristein, and S.M. Girvin, Phys. Rev. Lett. **64**, 587 (1990).

[12] Eli Ruckenstein and Nae-Lih Wu, in *Thallium-Based High Temperature Superconductors*, edited by A. Herman and J. V. Yakhmi (Marcel Dekker, New York, 1994), p. 119.

[13] A.F. Khoder, M. Couach, and B. Barbara, Physica C **153–155**, 1477 (1988).

[14] P. Chowdhury, Ph.D. thesis, Indian Institute of Technology, 2000.

[15] S. Gupta, R. Suba, B.D. Padalia, O. Prakash, R.M. Nayak, I.K. Gopalakrishan, and J.V. Yakhmi, Physica C **292**, 183 (1997).

[16] M. Gasgnier, L. Eyring, R.C. Karnatak, H. Dexpert, J.M. Esteva, P. Caro, and L. Albert, J. Less-Common Met. **127**, 367 (1987).

[17] Y. Shimakawa, Y. Kubo, T. Manako, and H. Igarashi, Phys. Rev. B **40**, 11 400 (1989).

[18] S.D. Obertelli, J.R. Cooper, and J.L. Tallon, Phys. Rev. B **46**, 14 928 (1992).

[19] M.R. Presland, J.L. Tallon, R.G. Buckley, R.S. Liu, and N.E. Flower, Physica C **176**, 95 (1991).

[20] A.A. Abrikosov and G. Gorkov, Zh. Éksp. Teor. Fiz. **39**, 1781 (1960) [Sov. Phys. JETP **12**, 1243 (1961)].

[21] N. F. Mott and E. A. Davis, in *Electronic Processes in Non-Crystalline Materials* (Clarendon Press, Oxford, 1971).

[22] U. Gottwick, K. Gloos, S. Horn, F. Steglich, and N. Grewe, J. Magn. Magn. Mater. **47**, 536 (1985).

[23] V.E. Gasumyants, N.V. Ageev, E.V. Vladimirskaya, V.I. Smirnov, A.V. Kazanskiy, and V.I. Kaydanov, Phys. Rev. B **53**, 905 (1996).

[24] S.J. Liu and W. Guan, Phys. Rev. B **58**, 11 716 (1998).

[25] P. Chowdhury and S.N. Bhatia, Physica C **319**, 150 (1999).

[26] X.H. Chen, T.F. Li, M. Yu, K.Q. Ruan, C.Y. Wang, and L.Z. Cao, Physica C **290**, 317 (1997).

[27] S. Keshri, J.B. Mandal, P. Mandal, A. Poddar, A.N. Das, and B. Ghosh, Phys. Rev. B **47**, 9048 (1993).

[28] S. Ikegawa, T. Wada, T. Yamashita, A. Ichinose, K. Matsuura, K. Kubo, H. Yamauchi, and S. Tanaka, Phys. Rev. B **43**, 11 508 (1991).

[29] I. P. Zvygin, in *Hopping Conduction in Solids*, edited by M. Pollak and B. Shklovskii (North-Holland, Amsterdam, 1991), p. 147.

[30] D. Mandrus, L. Forro, C. Kendziora, and L. Mihaly, Phys. Rev. B **44**, 2418 (1991).

[31] A. Junod, D. Eckert, G. Triscone, V.Y. Lee, and J. Muller, Physica C **159**, 215 (1989).

[32] P.A. Lee and T.V. Ramakrishnan, Rev. Mod. Phys. **57**, 287 (1985).

[33] S. Doniach and M. Inui, Phys. Rev. B **41**, 6668 (1990).

[34] J.A. Veira and F. Vidal, Physica C **159**, 468 (1989).

[35] S.N. Bhatia and C.P. Dhard, Phys. Rev. B **49**, 12 206 (1994).

[36] R. Fehrenbacher and T.M. Rice, Phys. Rev. Lett. **70**, 3471 (1993).